Chaos
An Interdisciplinary Journal of Nonlinear Science

RESEARCH ARTICLE | JANUARY 02 2026

The effect of parameter drift in the transport of magnetized plasma particles FREE

P. Haerter ; R. L. Viana

Check for updates

Chaos 36, 013105 (2026)
https://doi.org/10.1063/5.0302695

View Online
Export Citation

Articles You May Be Interested In

Chaotic transport in the drift motion for a magnetized plasma with nonlinear mode coupling

Phys. Plasmas (July 2025)

Eigenmode characterizations of slab ion-temperature-gradient instabilities in various magnetic shear configurations

AIP Advances (May 2021)

On the timescales in the chaotic dynamics of a 4D symplectic map

Chaos (October 2024)

20 January 2026 14:24:20

AIP Advances
Why Publish With Us?
21DAYS average time to 1st decision
OVER 4 MILLION views in the last year
INCLUSIVE scope
Learn More
AIP Publishing

AIP Publishing

The effect of parameter drift in the transport of magnetized plasma particles

Cite as: Chaos 36, 013105 (2026); doi: 10.1063/5.0302695
Submitted: 16 September 2025 · Accepted: 12 December 2025 ·
Published Online: 2 January 2026

View Online Export Citation CrossMark

P. Haerter[1,a] and R. L. Viana[1,2]

AFFILIATIONS

[1]Departamento de Física, Universidade Federal do Paraná, Curitiba 81531-990, Paraná, Brazil
[2]Centro Interdisciplinar de Ciência, Tecnologia e Inovação, Núcleo de Modelagem e Computação Científica, Universidade Federal do Paraná, Curitiba 81531-990, Paraná, Brazil

[a]**Author to whom correspondence should be addressed:** haerter@ufpr.br

ABSTRACT

We investigate how time dependent modulations of drift wave amplitudes affect particle transport and chaos in a magnetized plasma. Using the Horton model, we apply a sawtooth ramp to a primary wave's amplitude and periodic rectangular kicks to secondary waves, simulating a driven system. Particle transport is quantified by the mean square displacement exponent, α, and chaos by the maximum Lyapunov exponent. Our primary finding is a strong negative correlation between the system's average chaoticity and its transport efficiency. We show that rapid sawtooth ramping (short period τ) produces highly efficient, superdiffusive transport ($\alpha > 1$). In contrast, slower ramping increases the system's chaos but suppresses transport, driving it toward normal diffusion ($\alpha \to 1$). This counterintuitive result demonstrates that heightened chaos destroys the coherent, streamer like structures necessary for superdiffusive flights. Our findings indicate that the coherence of the turbulent field, rather than its raw chaoticity, is the key determinant of transport efficiency, offering a new perspective on plasma control.

Published under an exclusive license by AIP Publishing. https://doi.org/10.1063/5.0302695

20 January 2026 14:24:20

Using a driven Horton drift wave model with a sawtooth-ramped primary wave and kicked secondary waves, we show that slower ramping increases system-wide chaos but suppresses transport from a superdiffusive to a normal diffusive regime. This suppression occurs because heightened chaos destroys the coherent, streamer-like structures that are essential for efficient, long-range particle flights. Our findings establish that the temporal coherence of the turbulent field, not its raw chaoticity, is the key determinant of transport efficiency, offering a new perspective on plasma control.

I. INTRODUCTION

Achieving sustained nuclear fusion in magnetic confinement devices, such as tokamaks, requires overcoming the challenge of anomalous transport, where turbulent fluctuations drive particles and energy out of the plasma core much faster than classical theories predict.[1–6] This turbulence is often driven by low frequency electrostatic drift waves at the plasma edge,[7] which generate stochastic electric fields and induce chaotic particle motion via the $\mathbf{E} \times \mathbf{B}$ drift.[8,9] Cyclical magnetohydrodynamic (MHD) events in the plasma core, such as the sawtooth instability, can act as a natural pump, periodically expelling energy that modulates the conditions driving this edge turbulence.[10,11]

Historically, plasma turbulence was often viewed as a source of purely random, diffusive transport. However, a more modern understanding reveals that turbulence can self-organize into coherent structures that profoundly regulate transport.[4,12,13] These structures include zonal flows, poloidally symmetric sheared flows that can act as transport barriers, and streamers, which are radially elongated convective cells that create rapid transport highways.[14,15] The overall confinement efficiency is, therefore, determined by the complex competition between the randomizing effect of chaos and the formation of these ordered, coherent structures. Indeed, the study of chaotic particle trajectories and their relation to coherent structures remains a key topic in modern transport research.[16–20]

While classical transport is described by a linear growth of the mean square displacement (MSD) with time, anomalous diffusion is characterized by a non-linear scaling law, often arising in complex, heterogeneous systems.[21] This phenomenon is not unique to plasmas, and it has been extensively observed in diverse contexts

Published under an exclusive license by AIP Publishing

ranging from biological transport in crowded cellular environments to diffusion in porous media and chaotic dynamics in Hamiltonian systems.[22–26] In these systems, the breakdown of the central limit theorem—often due to long-range correlations or broad jump distributions—leads to superdiffusive (or even hyperdiffusive) behavior, where particles spread significantly faster than in normal Brownian motion.

In this work, we investigate how the temporal dynamics of drift wave amplitudes, motivated by these cyclical plasma phenomena, govern the balance between chaotic and coherent transport. We employ the Horton drift wave model[27] as our framework but introduce a crucial extension: we impose time dependent modulations on the wave amplitudes to mimic the energy dynamics of a driven dissipative system. Specifically, the primary wave's amplitude is modulated by a sawtooth ramp, representing a slow, periodic energy pump. The secondary waves are modulated by periodic rectangular pulses, modeling fast, intermittent energy transfer between modes, a scenario analogous to nonlinear three-wave interactions.[28,29] This approach allows us to explore how the interplay between slow pumping and fast kicks dictates the resulting transport regime.

Our analysis, based on parameters relevant to experimental devices, such as the Tokamak Chauffage Alfvén Brésilien (TCABR) tokamak,[30–32] reveals two distinct transport regimes. We find that rapid sawtooth ramping (short period τ) promotes the formation of coherent, streamer like transport channels, leading to highly efficient, superdiffusive motion ($\alpha > 1$). In contrast, slower ramping (long period τ) increases the chaoticity of the wave field. This heightened chaos disrupts the streamers, breaking the long-range correlation of particle trajectories and driving the system toward less efficient, normal diffusion ($\alpha \to 1$). Our central finding is, therefore, a strong negative correlation between the degree of chaos and the efficiency of anomalous transport, underscoring the critical role of wave field coherence in plasma confinement.[28]

This paper is structured as follows: Sec. II details the time dependent drift wave model. Section III presents the analysis of particle transport via the mean square displacement. Section IV provides the chaos analysis using the maximum Lyapunov exponent (MLE) and connects it to the observed transport regimes. Finally, Sec. V summarizes our findings and their implications for controlling transport in magnetized plasmas.

II. DRIFT WAVE MODEL

The dynamics of particles subjected to sawtooth wave pumping can be described by multiple models. For particles at the plasma edge, the model proposed by Horton is particularly suitable.[27] In this region, by neglecting curvature effects, the toroidal geometry can be locally approximated by a Cartesian slab. We, therefore, transform the toroidal coordinates (r, θ, ϕ) into a Cartesian system (x, y, z), where x represents the radial, y the poloidal, and z the toroidal directions, as illustrated in Fig. 1. The uniform magnetic field is directed along the z axis, given by $\vec{B} = B_0\hat{z}$.

We assume that the ion and electron charges do not appreciably affect the electric and magnetic fields; hence, the corresponding guiding centers can be considered passive tracers or test particles.

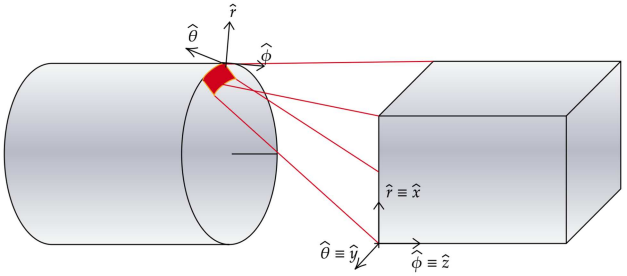


FIG. 1. Graphical representation of the transformation of cylindrical coordinates to rectangular ones.

Such test particles move with the $\mathbf{E} \times \mathbf{B}$ drift velocity,

$$\mathbf{v} = -\frac{\nabla\Phi \times \mathbf{B}}{B^2}, \tag{1}$$

where the electric field is written as $\mathbf{E} = -\nabla\Phi$, with $\Phi(x, y, t)$ being a scalar potential. This system is equivalent to the following set of canonical equations:

$$v_x = \frac{\mathrm{d}x}{\mathrm{d}t} = -\frac{1}{B_0}\frac{\partial\Phi}{\partial y}, \tag{2}$$

$$v_y = \frac{\mathrm{d}y}{\mathrm{d}t} = \frac{1}{B_0}\frac{\partial\Phi}{\partial x}, \tag{3}$$

corresponding to the time dependent Hamiltonian

$$H(x, y, t) = \frac{1}{B_0}\Phi(x, y, t). \tag{4}$$

While the underlying instability generating these drift waves in the tokamak edge is often collisional in nature, we adopt a collisionless guiding-center approximation for the particle trajectories, implicitly assuming that the collision time exceeds the characteristic timescales of the chaotic transport. We assume that the ion and electron charges do not appreciably affect the electric and magnetic fields;[27] hence, the corresponding guiding centers can be considered passive tracers, or test particles, evolved by Eqs. (2) and (3).

The electric potential can be divided into two parts: an equilibrium part $\Phi_0(x)$ corresponding to a radial electric field and a perturbation caused by N drift waves with amplitudes A_i, frequencies ω_i, and wave vectors $\mathbf{k}_i = (k_{x,i}, k_{y,i})$ for $i = 1, 2, \ldots, N$. This gives

$$\Phi(x, y, t) = \Phi_0(x) + \sum_{i=1}^{N} A_i \sin(k_{x,i}x + \beta_i)\cos(k_{y,i}y - \omega_i t), \tag{5}$$

where we assume a stationary wave pattern along the radial direction x and a traveling wave along the poloidal direction y. Let L_x and L_y be the characteristic lengths along these directions such that

$$k_x = \frac{n\pi}{L_x}, \quad k_y = \frac{2\pi m}{L_y}, \tag{6}$$

where m and n are suitably chosen positive integers.

20 January 2026 14:24:20

Published under an exclusive license by AIP Publishing

In the case of N drift waves, the Hamiltonian reads

$$H(x,y,t) = \frac{1}{B_0}\left[\Phi_0(x) + \sum_{i=1}^{N} A_i \sin(k_{x,i}x + \beta_i)\cos(k_{y,i}y - \omega_i t)\right]. \tag{7}$$

After transitioning to a reference frame moving with the phase velocity of the first wave, u_1, and considering the resonant case where the drift velocity satisfies

$$v_e = \frac{1}{B}\frac{\mathrm{d}\Phi_0}{\mathrm{d}x} = u_1 = \frac{\omega_1}{k_{y,1}},$$

the Hamiltonian becomes

$$H(x,y,t) = A_1 \sin(k_{x,1}x)\cos(k_{y,1}y) + \sum_{i=2}^{N} A_i \sin(k_{x,i}x + \beta_i)\cos\left(k_{y,i}(y - u_i t)\right), \tag{8}$$

where $u_i = \frac{\omega_i}{k_{y,i}} - \frac{\omega_1}{k_{y,1}}$ and $\beta_i = \pi/2$ is a phase term associated with the breakdown of transport barriers in symmetry regions. This phase enables particle transport along the x-direction, which is the focus of this study.[33]

The sawtooth pumping[11] is introduced by modulating the amplitude of the reference wave, A_1, as follows:

$$A_1(t) = A_{1,\max}\frac{t \pmod{\tau}}{\tau}, \tag{9}$$

where $A_{1,\max}$ is the maximum amplitude (set to 1.0 in this work) and τ is the period of the sawtooth ramp.

Simultaneously, the amplitudes of the other waves (A_i for $i > 1$) are modulated as periodic rectangular pulses to represent energy exchange between modes.[29] Their amplitude is given by

$$A_{i>1}(t) = \begin{cases} A_{i,\max} & \text{if } t \pmod{\tau} \le \dfrac{\tau}{\nu}, \\ 0 & \text{otherwise}, \end{cases} \tag{10}$$

where $A_{i,\max}$ is the maximum amplitude of the pulse, τ is the period, and the parameter ν controls the pulse width, $W = \tau/\nu$.

Physically, this modulation represents the arrival of a heat pulse at the plasma edge, generated by a sawtooth crash in the core. While the sawtooth instability itself is a magnetic reconnection event in the core, the energy it expels propagates radially, transiently steepening the edge gradients and acting as a pump for the electrostatic turbulence.[10]

The choice of system parameters is directly motivated by experimental observations from the TCABR tokamak. Measurements of the potential edge fluctuations using electrostatic probes indicate a poloidal wave number k_θ in the range of (1–5) $\times 10^3\ \mathrm{m}^{-1}$, with a broad spectral content and a pronounced feature at $\omega_{\exp} \approx 50$ kHz.[29,32,34,35]

Based on the dominant poloidal wave number of these plasma edge fluctuations, we fix the primary wave vector at $k_\theta = k_{y,1} = 3 \times 10^3\ \mathrm{m}^{-1}$. In our normalized units (where lengths are scaled by the characteristic scale $L_n \approx \rho_s$), this corresponds to a dimensionless wavenumber of $k_{y,1} \approx 3$.[29]

To determine the dimensionless frequencies, we scale the experimental frequency $\omega_{\exp}$ by the ion-cyclotron frequency Ω_{ci}, adjusted by the wavenumber order. This yields a normalized frequency of $\omega \approx 0.476$. Consequently, we set $\omega_1 = \omega_2 = \omega_3 = 0.476$. It is important to note that because we fix the frequencies to this dominant experimental spectral feature, the strict three-wave frequency resonance condition ($\omega_1 + \omega_2 = \omega_3$) is not enforced.[36] The waves, therefore, act as driven quasi-modes typical of a fully developed turbulent state.

The resulting system parameters are

$$k_{x,1} = 5, \quad k_{y,1} = 3, \quad \omega_1 = 0.476, \quad A_1 = 1.0,$$
$$k_{x,2} = -3, \quad k_{y,2} = -1.5, \quad \omega_2 = 0.476, \quad A_2 = 0.1,$$
$$k_{x,3} = -2, \quad k_{y,3} = -1.5, \quad \omega_3 = 0.476, \quad A_3 = 0.033.$$

Considering three modes[37] in the Hamiltonian equation (8), we evolved the canonical equations (2) and (3) numerically from $t_i = 0$ to $t_f = 10^4$, with τ (the ramping period) and ν (the duration of the kicks) serving as a tunable parameter. The representation of the waves amplitudes can be seen in Fig. 2.

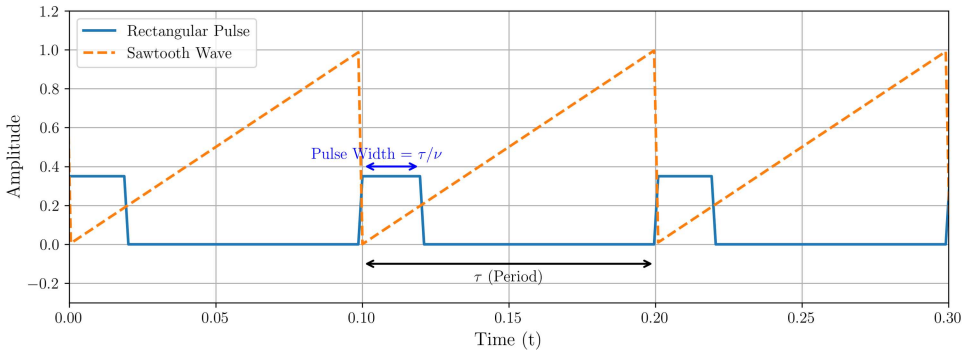


FIG. 2. Time evolution of the modulated wave amplitudes. The dashed orange line shows the sawtooth modulation of the primary wave amplitude, $A_1(t)$, with period τ. The solid blue line shows the rectangular pulse modulation for the secondary wave amplitudes, $A_{i>1}(t)$, which represents periodic kicks to the system.

20 January 2026 14:24:20

Published under an exclusive license by AIP Publishing

III. PARTICLE TRANSPORT

To analyze the transport dynamics induced by the different combinations of ramping and pulse parameters, we simulated an ensemble of passive particles initially distributed uniformly in the domain $x \in [-\pi, \pi]$ and $y \in [-2\pi, 2\pi]$.[38] We employed the mean square displacement (MSD) to provide a global characterization of the chaotic transport by quantifying the spatial spread of particles over time.

A. Mean square displacement

For a statistical characterization of transport, we computed the mean square displacement (MSD) in the radial direction,

$$\langle \sigma_x(t)^2 \rangle = \frac{1}{M} \sum_{i=1}^{N} |x_i(t) - x_i(0)|^2, \tag{11}$$

where M is the total number of particles. The long term behavior of the MSD scales with time as $\langle \sigma_x(t)^2 \rangle \propto t^\alpha$, where the scaling exponent α classifies the transport regime.[21] The regimes are subdiffusive ($\alpha < 1$), normal diffusion ($\alpha = 1$), superdiffusive ($1 < \alpha < 2$), or ballistic ($\alpha = 2$). An exponent of $\alpha > 2$ is sometimes referred to as hyperdiffusive.

Our analysis, summarized in Fig. 3, reveals a strong dependence of the transport regime on the sawtooth period τ. For short ramping periods (small τ), the particles exhibit highly enhanced, superdiffusive transport, with scaling exponents α approaching 2.0. As the ramping period τ increases, the transport is consistently suppressed, and the scaling exponent α trends toward 1.0, indicative of normal diffusion. This demonstrates that the system's transport properties can be effectively tuned from a superdiffusive or even hyperdiffusive state down to a standard diffusive process simply by adjusting the ramping frequency of the primary wave.

The parameter ν, which controls the duration of the rectangular pulse kicks ($W = \tau/\nu$), also has a notable effect on the transport. Figure 3 shows that shorter kicks (corresponding to larger ν) generally lead to slightly higher values of the transport exponent α. While shorter, the kicks still inject energy into the system, and their interaction with the primary ramping wave appears crucial for generating the most efficient transport.

Interestingly, this combination is a necessary mechanism for the emergence of the hyperballistic regime ($\alpha \geq 2$). It has been shown in the previous work[38] that a simpler model—one with a constant amplitude primary wave and suppressed secondary waves—only produces standard superdiffusive transport ($1 < \alpha < 2$). Therefore, the interplay between the slow sawtooth ramp of the main wave and the fast, periodic kicks from the other waves is the key physical process that gives rise to the hyperballistic motion observed in our results.

The observed transport regimes can be understood by considering the underlying phase space structure. The highly superdiffusive transport at small τ suggests the presence of coherent structures that allow for long, correlated particle flights. The rapid sawtooth ramp likely accelerates particles along preferential pathways before they can be fully randomized. In contrast, as the ramping period τ increases, the slower but more sustained perturbations lead to the widespread destruction of these coherent pathways. This enhanced chaos, which we will quantify in Sec. IV, disrupts the long-range correlations, causing particles to undergo more random, diffusive motion and thus suppressing the overall transport efficiency ($\alpha \to 1$).

IV. MAXIMUM LYAPUNOV EXPONENT

The time dependent Hamiltonian system described by Eq. (8) is non integrable, and as such, it exhibits chaotic dynamics for certain

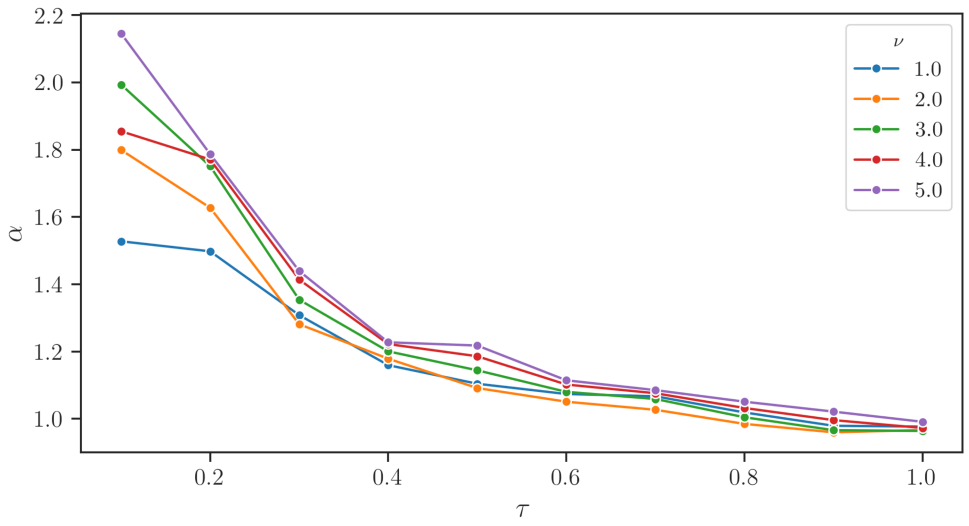


FIG. 3. The MSD scaling exponent α as a function of the sawtooth wave period (τ) for different values of the kick duration parameter (ν). The plot demonstrates a clear suppression of anomalous transport (i.e., α approaches 1) as the ramping period τ is increased.

20 January 2026 14:24:20

Published under an exclusive license by AIP Publishing

parameter ranges.[39] The degree of this chaos can be quantified by measuring the average rate of separation of initially close trajectories in phase space. This rate is given by the Maximum Lyapunov Exponent (MLE), denoted by λ. For a given trajectory, the MLE is defined as

$$\lambda = \lim_{t\to\infty} \frac{1}{t} \ln \frac{\|\delta\mathbf{x}(t)\|}{\|\delta\mathbf{x}(0)\|}, \tag{12}$$

where $\|\delta\mathbf{x}(t)\|$ is the magnitude of the separation vector between two initially close trajectories at time t.[40,41] A positive MLE ($\lambda > 0$) is a hallmark of chaos, indicating exponential divergence of trajectories and sensitive dependence on initial conditions. Conversely, a value of $\lambda \leq 0$ signifies regular, nonchaotic motion.

Numerically, the MLE was computed using the standard Benettin algorithm.[42] This method involves evolving a tangent vector $\delta\mathbf{x}$ via the linearized equations of motion alongside the non-linear trajectory. To avoid numerical overflow due to the exponential divergence, the tangent vector is re-normalized at regular time intervals. The finite-time Lyapunov exponent is then obtained by averaging the logarithmic growth rates of the vector norm over the simulation duration.

To visualize the structure of the phase space, we computed the MLE for a grid of initial conditions, as shown in the colormaps of Fig. 4. In these plots, regions of regular, quasiperiodic motion (e.g., stable islands) correspond to low λ values (bright yellow), while the chaotic sea is characterized by high λ values (dark blue/purple).

The plots reveal clear trends with respect to the control parameters. As the sawtooth period τ is increased [Figs. 4(d)–4(f)], the dark, chaotic sea expands and intensifies, encroaching upon the stable yellow islands. Conversely, as the kick duration is made shorter by increasing ν [Figs. 4(a)–4(c)], the yellow regions of regular motion become more prominent, indicating a less chaotic system overall.

A statistical overview of these trends is presented in the violin plots of Fig. 5. Unlike standard box plots, violin plots illustrate the full probability density of the data: the width of the shaded area at a given λ represents the relative frequency of particles possessing that Lyapunov exponent. This visualization facilitates the inference of the underlying phase space topology directly from the shape of the distribution.

In Fig. 5, each panel corresponds to a fixed kick parameter ν, while the distributions for varying sawtooth periods τ are displayed. A clear trend is observed as the ramping period increases. For small τ, the distributions are often "bottom-heavy" (broadening near $\lambda \approx 0$), indicating that a significant fraction of the ensemble is trapped in regular, sticky regions of phase space. These are the trajectories responsible for the superdiffusive transport. However, as τ increases, the distributions shift toward higher λ and become "top-heavy." This transformation reflects the destruction of stable islands and the homogenization of the chaotic sea as the driving becomes slower and more sustained. Comparing the panels reveals the secondary effect: panels corresponding to higher ν (shorter kicks) maintain the bottom-heavy, regularized shape for a wider range of τ compared to panels with low ν.

Complementing the distributional analysis, Fig. 6 aggregates the data into box plots to quantify the global trends of the mean

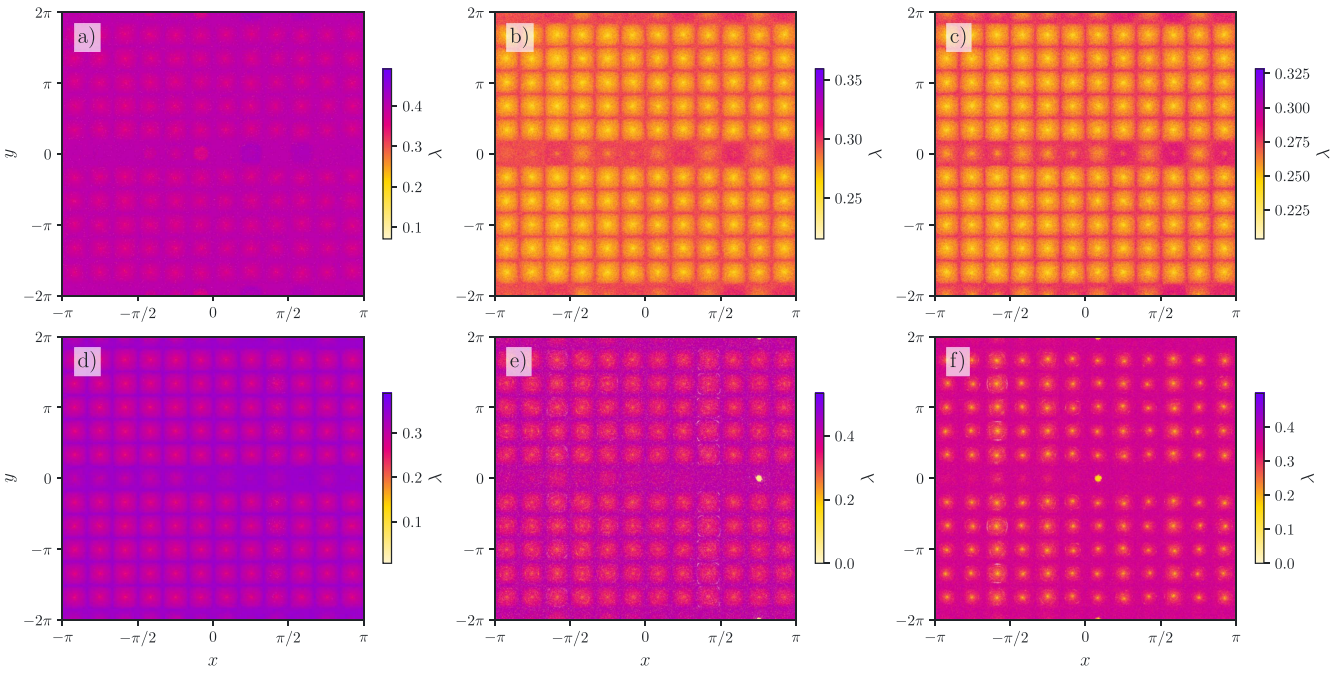


FIG. 4. Colormaps of the maximum Lyapunov exponent (λ) in the system phase space for fixed $\tau = 0.1$ and varying ν in the top row: (a) $\nu = 1.0$, (b) $\nu = 3.0$, and (c) $\nu = 5.0$. The bottom row shows results for fixed $\nu = 5.0$ and varying τ: (d) $\tau = 0.2$, (e) $\tau = 0.4$, and (f) $\tau = 0.6$. The darker colors correspond to regular motion ($\lambda \approx 0$), and lighter colors indicate highly chaotic regions ($\lambda > 0$).

20 January 2026 14:24:20

Published under an exclusive license by AIP Publishing

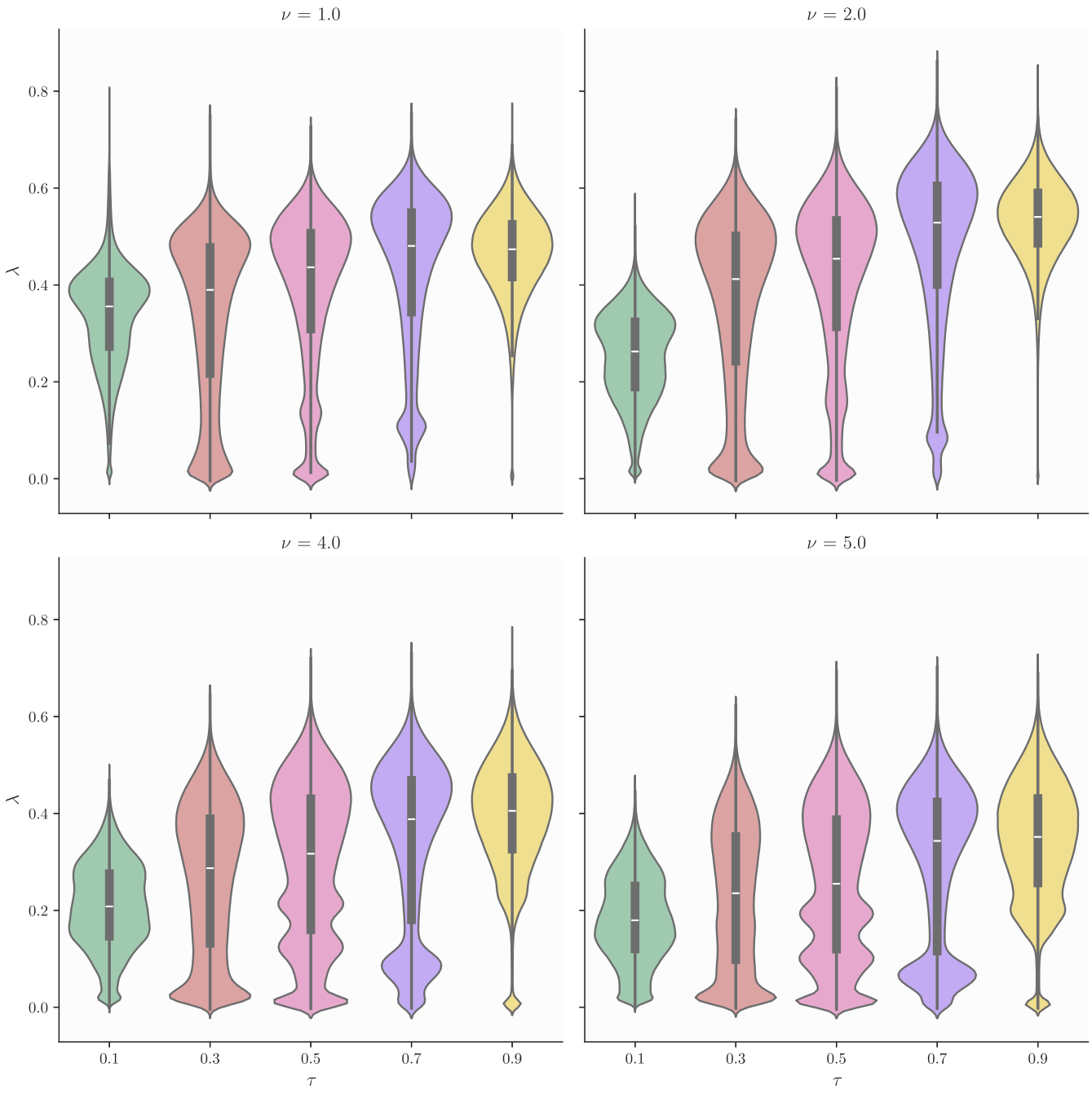


FIG. 5. Distributions of the maximum Lyapunov exponent (λ) plotted for different sawtooth ramping period (τ). The panels show results for fixed kick parameters: (a) $\nu = 1.0$, (b) $\nu = 2.0$, (c) $\nu = 4.0$, and (d) $\nu = 5.0$. The visual trend demonstrates that increasing τ shifts the bulk of the distribution toward higher positive values, corresponding to enhanced chaotic scattering. In contrast, higher values of ν (shorter kicks) maintain a significant population near $\lambda \approx 0$, indicating the persistence of regular, sticky regions in phase space that support superdiffusive transport.

maximum Lyapunov exponent, Λ. These plots provide a robust summary of the system average chaoticity, displaying the median, interquartile range, and outliers for the ensemble.

Two distinct monotonic trends are evident. First, Fig. 6(a) demonstrates a clear positive correlation between the sawtooth period τ and the average chaos Λ. Physically, a longer period implies

20 January 2026 14:24:20

Published under an exclusive license by AIP Publishing

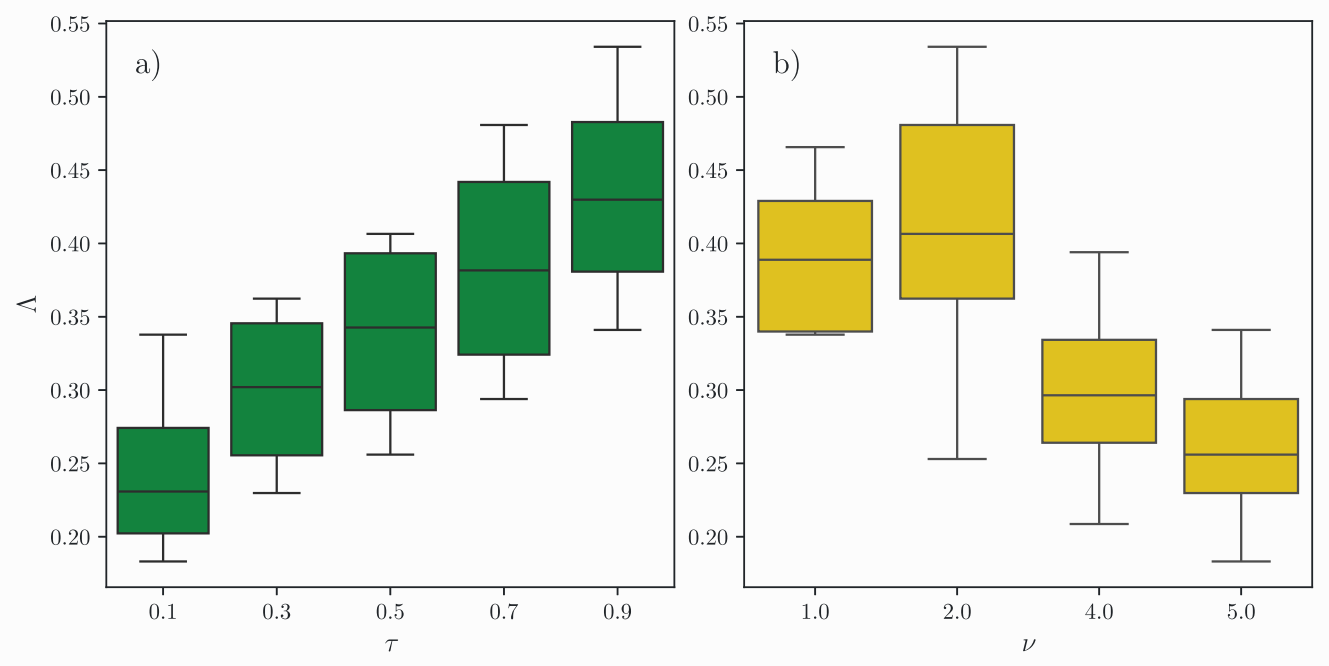


FIG. 6. Boxplots of the mean Lyapunov exponent, Λ. (a) Λ as a function of the ramping period τ. (b) Λ as a function of the kick parameter ν. The plots confirm that the average chaoticity of the system increases with τ and decreases with ν.

a slower, more sustained ramping of the primary wave amplitude. This slower evolution allows the perturbation to act coherently over longer timescales, effectively destroying the transport barriers and expanding the chaotic sea.

Second, Fig. 6(b) reveals a negative correlation between the kick parameter ν and Λ. Since the pulse width is defined as $W = \tau/\nu$, increasing ν corresponds to shortening the duration of the secondary wave kicks. The plot confirms that shorter, more impulsive kicks result in lower average chaoticity, allowing the system to retain more regular, stable orbits. Together, these results establish that the degree of chaos in the plasma edge model is a highly tunable quantity, controllable via the temporal characteristics of the driving mechanism.

The central result of this paper is the relationship between the system average chaoticity, Λ, and the transport exponent, α. To quantify this relationship, two standard statistical metrics are used: the Pearson correlation coefficient (r), which measures the linear association between the variables, and the Spearman correlation coefficient (ρ), which measures the strength of a monotonic (not necessarily linear) relationship.

As shown in the scatterplot of Fig. 7, there is a strong negative correlation between these two quantities (Pearson $r = -0.78$, Spearman $\rho = -0.84$). This indicates that more chaotic systems produce less anomalous transport. The high negative values of both coefficients provide robust statistical confirmation

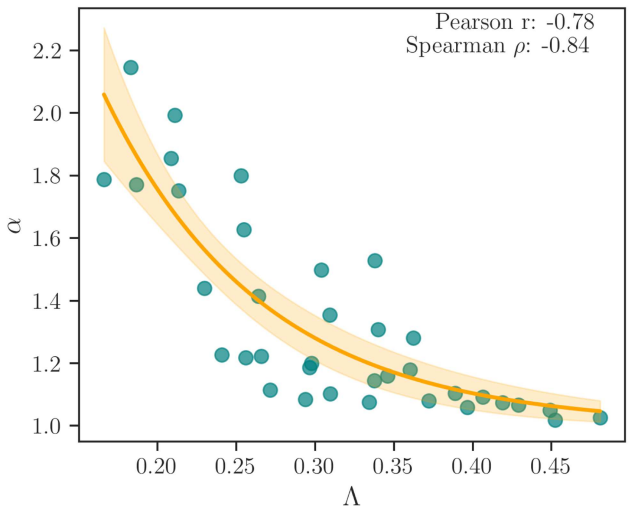


FIG. 7. Scatterplot showing the relationship between the mean Lyapunov exponent (Λ) and the transport exponent (α). The strong negative correlation indicates that more chaotic systems exhibit less anomalous transport (i.e., α is closer to 1). The orange line is a best fit curve, with the shaded region representing the 95% confidence interval.

20 January 2026 14:24:20

Published under an exclusive license by AIP Publishing

of the visual trend. This result demonstrates that as the average Lyapunov exponent increases—indicating the destruction of regular structures—the transport regime is consistently suppressed from superdiffusive (high α) toward normal diffusion ($\alpha \to 1$).

This seemingly counter-intuitive result is explained by the disruption of coherent structures in phase space, a phenomenon statistically demonstrated by the λ distributions in Fig. 5. For systems with low chaos (low τ, high ν), the "bottom-heavy" distributions in Fig. 5 confirm the presence of stable, sticky regions that allow particles to engage in long, correlated flights along stable manifolds, leading to superdiffusive motion (high α). However, as chaos increases (high τ, low ν), Fig. 5 shows that these low-λ regions are reduced. Particles are scattered more effectively throughout the chaotic sea, where their motion can resemble a classic random walk. This destruction of long-range correlation suppresses the transport efficiency, driving the system toward a state of normal diffusion ($\alpha \to 1$).

V. CONCLUSIONS

In this work, we investigated the impact of time dependent wave amplitude modulations on particle transport and chaos in a magnetized plasma. By extending the Horton drift wave model to include a primary wave driven by a slow sawtooth ramp and secondary waves subjected to fast, periodic kicks, we simulated a dynamic environment analogous to a driven dissipative system. Using the Mean Square Displacement (MSD) and the Maximum Lyapunov Exponent (MLE) as our primary diagnostics, we systematically explored the effects of the ramping period (τ) and the kick duration parameter (ν).

Our central finding is that the transport regime is highly tunable and exhibits a strong, counterintuitive negative correlation with the system's chaoticity. We demonstrated that rapid sawtooth ramping (small τ) facilitates highly efficient, superdiffusive transport ($\alpha > 1$), which can even enter a hyperballistic regime. Conversely, slower ramping (large τ) increases the overall chaos in the system but suppresses anomalous transport, driving the scaling exponent toward that of normal diffusion ($\alpha \to 1$).

This result is explained by the competition between chaos and the formation of coherent transport structures. In less chaotic regimes, particles can follow streamer like channels, leading to long, correlated flights and superdiffusive behavior. As the system becomes more chaotic, these coherent pathways are destroyed. The increased scattering randomizes particle trajectories, disrupting the mechanism for efficient transport and resulting in a classic diffusive process. This highlights a crucial insight: simply increasing the chaoticity of the driving fields does not necessarily enhance transport; instead, it can suppress it by destroying the underlying coherence that enables it.

The findings have significant implications for controlling plasma transport. They suggest that the nature of particle flux is not a fixed outcome of turbulence but can be actively manipulated by controlling the temporal characteristics of the driving instabilities. Modulating the frequency and form of energy injection into turbulent modes could offer a potential strategy to either enhance the flushing of impurities or suppress the transport of fuel particles to improve confinement. Future work could explore more complex and realistic modulation waveforms derived from advanced simulations or experimental data, as well as incorporate the effects of magnetic field fluctuations to build a more comprehensive picture of transport regulation in magnetized plasmas.

ACKNOWLEDGMENTS

This work has been supported by grants from the Brazilian Government Agencies CNPq and CAPES. P. Haerter received partial financial support from the following Brazilian government agencies: CNPq (140920/2022-6) and CAPES (88887.898818/2023-00). R. L. Viana received partial financial support from the following Brazilian government agencies: CNPq (403120/2021-7, 301019/2019-3) and CAPES (88881.143103/2017-01).

AUTHOR DECLARATIONS

Conflict of Interest

The authors have no conflicts to disclose.

Author Contributions

P. Haerter: Conceptualization (equal); Data curation (equal); Formal analysis (equal); Funding acquisition (equal); Investigation (equal); Methodology (equal); Project administration (equal); Resources (equal); Software (equal); Validation (equal); Visualization (equal); Writing – original draft (equal); Writing – review & editing (equal). **R. L. Viana:** Conceptualization (equal); Data curation (equal); Formal analysis (equal); Funding acquisition (equal); Investigation (equal); Methodology (equal); Project administration (equal); Resources (equal); Supervision (equal); Validation (equal); Visualization (equal); Writing – original draft (equal); Writing – review & editing (equal).

DATA AVAILABILITY

The data that support the findings of this study are available within the article. The numerical code used to generate the data and figures is openly available in GitHub at https://github.com/pedro12374/Sawtooth-Plasma-Transport, Ref. 43.

REFERENCES

[1] B. Carreras, "Progress in anomalous transport research in toroidal magnetic confinement devices," IEEE Trans. Plasma Sci. **25**, 1281–1321 (1997).
[2] W. Horton, *Turbulent Transport in Magnetized Plasmas*, 2nd ed. (World Scientific, 2017).
[3] W. Horton, J.-H. Kim, E. Asp, T. Hoang, T.-H. Watanabe, and H. Sugama, "Drift wave turbulence," AIP Conf. Proc. **1013**, 1–19 (2008).
[4] R. Balescu, *Aspects of Anomalous Transport in Plasmas* (CRC Press, Boca Raton, FL, 2005).
[5] F. F. Chen, *Introduction to Plasma Physics and Controlled Fusion* (Springer International Publishing, Cham, 2016).
[6] X. Garbet, P. Mantica, C. Angioni, E. Asp, Y. Baranov, C. Bourdelle, R. Budny, F. Crisanti, G. Cordey, L. Garzotti, N. Kirneva, D. Hogeweij, T. Hoang, F. Imbeaux, E. Joffrin, X. Litaudon, A. Manini, D. C. McDonald, H. Nordman, V. Parail, A. Peeters, F. Ryter, C. Sozzi, M. Valovic, T. Tala, A. Thyagaraja, I. Voitsekhovitch, J. Weiland, H. Weisen, A. Zabolotsky, and the JET EFDA Contributors, "Physics of transport in tokamaks," Plasma Phys. Controlled Fusion **46**, B557–B574 (2004).
[7] W. Horton, "Drift waves and transport," Rev. Mod. Phys. **71**, 735–778 (1999).

20 January 2026 14:24:20

Published under an exclusive license by AIP Publishing

[8]S. J. Camargo, B. D. Scott, and D. Biskamp, "The influence of magnetic fluctuations on collisional drift-wave turbulence," Phys. Plasmas **3**, 3912–3931 (1996).
[9]A. Hasegawa and K. Mima, "Pseudo-three-dimensional turbulence in magnetized nonuniform plasma," Phys. Fluids **21**, 87–92 (1978).
[10]K. Zhao, Y. Nagashima, Z. Guo, P. H. Diamond, J. Dong, L. Yan, K. Itoh, S.-I. Itoh, X. Li, J. Li, A. Fujisawa, S. Inagaki, J. Cheng, J. Xu, Y. Kosuga, M. Sasaki, Z. Wang, H. Zhang, Y. Chen, X. Cao, D. Yu, Y. Liu, X. Song, F. Xia, and S. Wang, "Effects of sawtooth heat pulses on edge flows and turbulence in a tokamak plasma," Plasma Sci. Technol. **25**, 015101 (2023).
[11]J. A. Wesson, "Sawtooth oscillations," Plasma Phys. Controlled Fusion **28**, 243 (1986).
[12]P. H. Diamond, S.-I. Itoh, K. Itoh, and T. S. Hahm, "Zonal flows in plasma—A review," Plasma Phys. Controlled Fusion **47**, R35 (2005).
[13]P. W. Terry, "Suppression of turbulence and transport by sheared flow," Rev. Mod. Phys. **72**, 109–165 (2000).
[14]G. S. Xu, V. Naulin, W. Fundamenski, C. Hidalgo, J. A. Alonso, C. Silva, B. Gonçalves, A. H. Nielsen, J. Juul Rasmussen, S. I. Krasheninnikov, B. N. Wan, M. Stamp, and JET EFDA Contributors, "Blob/hole formation and zonal-flow generation in the edge plasma of the JET tokamak," Nucl. Fusion **49**, 092002 (2009).
[15]B. D. Scott, "Energetics of the interaction between electromagnetic $\mathbf{E} \times \mathbf{B}$ turbulence and zonal flows," New J. Phys. **7**, 92 (2005).
[16]M. V. Falessi, F. Pegoraro, and T. J. Schep, "Lagrangian coherent structures and plasma transport processes," J. Plasma Phys. **81**, 495810505 (2015).
[17]F. A. Marcus, I. L. Caldas, Z. O. Guimarães-Filho, P. J. Morrison, W. Horton, Yu. K. Kuznetsov, and I. C. Nascimento, "Reduction of chaotic particle transport driven by drift waves in sheared flows," Phys. Plasmas **15**, 112304 (2008).
[18]G. Sonnino, P. Nardone, P. Peeters, and E. Tirapegui, "Nonlinear transport in nonequilibrium systems (with an application to tokamak-plasmas)," Chaos **30**, 063110 (2020).
[19]L. A. Osorio, M. Roberto, I. L. Caldas, R. L. Viana, and Y. Elskens, "Onset of internal transport barriers in tokamaks," Phys. Plasmas **28**, 082305 (2021).
[20]B. F. McMillan, C. C. T. Pringle, and B. Teaca, "Simple advecting structures and the edge of chaos in subcritical tokamak plasmas," J. Plasma Phys. **84**, 905840611 (2018).
[21]R. Metzler and J. Klafter, "The random walk's guide to anomalous diffusion: A fractional dynamics approach," Phys. Rep. **339**, 1–77 (2000).
[22]G. Zaslavsky, "Chaos, fractional kinetics, and anomalous transport," Phys. Rep. **371**, 461–580 (2002).
[23]J. D. Meiss, N. Miguel, C. Simó, and A. Vieiro, "Accelerator modes and anomalous diffusion in 3D volume-preserving maps," Nonlinearity **31**, 5615–5642 (2018).
[24]*Chaos, Kinetics and Nonlinear Dynamics in Fluids and Plasmas: Proceedings of a Workshop Held in Carry-le Rouet, France, 16–21 June 1997*, Lecture Notes in Physics Vol. 511, edited by S. Benkadda, G. M. Zaslavsky, H. Araki, R. Beig, J. Ehlers, U. Frisch, K. Hepp, R. L. Jaffe, R. Kippenhahn, H. A. Weidenmüller, J. Wess, J. Zittartz, and W. Beiglböck (Springer, Berlin, 1998).
[25]I. Golding and E. C. Cox, "Physical nature of bacterial cytoplasm," Phys. Rev. Lett. **96**, 098102 (2006).
[26]A. Cortis and J. Birkholzer, "Continuous time random walk analysis of solute transport in fractured porous media," Water Resour. Res. **44**, 2007WR006596, https://doi.org/10.1029/2007WR006596 (2008).
[27]W. Horton, "Onset of stochasticity and the diffusion approximation in drift waves," Plasma Phys. Controlled Fusion **27**, 937 (1985).
[28]P. Haerter, I. L. Caldas, and R. L. Viana, "Chaotic transport in the drift motion for a magnetized plasma with nonlinear mode coupling," Phys. Plasmas **32**, 072307 (2025).
[29]A. M. Batista, I. L. Caldas, S. R. Lopes, R. L. Viana, W. Horton, and P. J. Morrison, "Nonlinear three-mode interaction and drift-wave turbulence in a tokamak edge plasma," Phys. Plasmas **13**, 042510 (2006).
[30]I. C. Nascimento, Y. K. Kuznetsov, J. H. F. Severo, A. M. M. Fonseca, A. Elfimov, V. Bellintani, M. Machida, M. V. A. P. Heller, R. M. O. Galvão, E. K. Sanada, and J. I. Elizondo, "Plasma confinement using biased electrode in the TCABR tokamak," Nucl. Fusion **45**, 796 (2005).
[31]A. A. Ferreira, M. V. A. P. Heller, I. L. Caldas, E. A. Lerche, L. F. Ruchko, and L. A. Baccalá, "Turbulence and transport in the scrape-off layer TCABR tokamak," Plasma Phys. Controlled Fusion **46**, 669 (2004).
[32]R. M. Castro, M. V. A. P. Heller, I. L. Caldas, R. P. da Silva, Z. A. Brasilio, and I. C. Nascimento, "Temperature fluctuations and plasma edge turbulence in the Brazilian tokamak TBR," Phys. Plasmas **3**, 971–977 (1996).
[33]R. G. Kleva and J. F. Drake, "Stochastic $\mathbf{E} \times \mathbf{B}$ particle transport," Phys. Fluids **27**, 1686–1698 (1984).
[34]M. V. A. P. Heller, R. M. Castro, I. L. Caldas, Z. A. Brasílio, R. P. da Silva, and I. C. Nascimento, "Correlation between plasma edge electrostatic and magnetic oscillations in the Brazilian tokamak TBR," J. Phys. Soc. Jpn. **66**, 3453–3460 (1997).
[35]G. Z. dos Santos Lima, Z. O. Guimarães-Filho, A. M. Batista, I. L. Caldas, S. R. Lopes, R. L. Viana, I. C. Nascimento, and Yu. K. Kuznetsov, "Bicoherence in electrostatic turbulence driven by high magnetohydrodynamic activity in Tokamak Chauffage Alfvén Brésilien," Phys. Plasmas **16**, 042508 (2009).
[36]S. R. Lopes and A. C.-L. Chian, "Controlling chaos in nonlinear three-wave coupling," Phys. Rev. E **54**, 170–174 (1996).
[37]K. Katou, "Resonant three-wave interaction in electrostatic drift-wave turbulence," J. Phys. Soc. Jpn. **51**, 996–1000 (1982).
[38]P. Haerter, R. L. Viana, and E. D. Leonel, "Escape and transport in chaotic motion of charged particles in a magnetized plasma under the influence of two and three modes of drift waves," Chaos, Solitons Fractals **200**, 117162 (2025).
[39]A. C. Mathias, R. L. Viana, T. Kroetz, and I. L. Caldas, "Fractal structures in the chaotic motion of charged particles in a magnetized plasma under the influence of drift waves," Physica A **469**, 681–694 (2017).
[40]A. J. Lichtenberg and M. A. Lieberman, *Regular and Chaotic Dynamics*, Applied Mathematical Sciences Vol. 38 (Springer, New York, 1992).
[41]E. Ott, *Chaos in Dynamical Systems*, 2nd ed. (Cambridge University Press, Cambridge, 2002).
[42]G. Benettin, L. Galgani, A. Giorgilli, and J.-M. Strelcyn, "Lyapunov characteristic exponents for smooth dynamical systems and for Hamiltonian systems; a method for computing all of them. Part 1: Theory," Meccanica **15**, 9–20 (1980).
[43]P. Haerter (2025). "Sawtooth-plasma-transport," Github, https://github.com/pedro12374/Sawtooth-Plasma-Transport.

20 January 2026 14:24:20

Published under an exclusive license by AIP Publishing